

Exact zeros of Loschmidt echo and quantum speed limit time for dynamical quantum phase transition in finite size systems

Bozhen Zhou,^{1,2} Yumeng Zeng,^{1,2} and Shu Chen^{1,2,3,*}

¹*Beijing National Laboratory for Condensed Matter Physics,
Institute of Physics, Chinese Academy of Sciences, Beijing 100190, China*

²*School of Physical Sciences, University of Chinese Academy of Sciences, Beijing 100049, China*

³*Yangtze River Delta Physics Research Center, Liyang, Jiangsu 213300, China*

(Dated: August 5, 2022)

We study exact zeros of Loschmidt echo and quantum speed limit time for dynamical quantum phase transition in finite size systems. Our results illustrate that exact zeros of Loschmidt echo exist even in finite size quantum systems when the postquench parameter takes some discrete values in regions with the corresponding equilibrium phase different from the initial phase. As the system size increases and tends to infinity, the discrete parameters distribute continuously in the parameter regions. We further analyse the first time for the appearance of the exact zero of Loschmidt echo which is known as the quantum speed limit time τ_{QSL} . We demonstrate that the maximal value of τ_{QSL} is proportional to L and approaches infinity in the thermodynamical limit, when we quench the initial non-critical state to the critical phase. We also calculate the minimal value of τ_{QSL} and find that its behaviour is dependent on the phase of initial state.

I. INTRODUCTION

In recent years, the development of quantum simulation platforms, such as neutral atom arrays^{1–4}, stimulates the intensive studies on the nonequilibrium dynamics of quantum many-body systems. An interesting issue is the dynamical quantum phase transition (DQPT)^{5–27}, which describes dynamical quantum critical phenomena presented in quench dynamics of kinds of quantum systems with initial state chosen as the ground state of a given Hamiltonian and evolving under a sudden change of a Hamiltonian parameter. The DQPT is characterized by the emergence of zero points of Loschmidt echo (LE) at a series of critical times, where the LE is defined by $\mathcal{L}(t) = |\mathcal{G}(t)|^2$ with the Loschmidt amplitude given by

$$\mathcal{G}(t) = \langle \psi_i | e^{-iH_f t} | \psi_i \rangle. \quad (1)$$

Here $|\psi_i\rangle$ is the ground state of prequench Hamiltonian and H_f is the postquench Hamiltonian. The LE measures the overlap between initial quantum state and time-evolved state²⁸, which has wide application in various contexts ranging from the theory of quantum chaos^{28–30} and the Schwinger mechanism of particle production^{31,32}, to work distribution functions in the context of nonequilibrium fluctuation theorems^{33,34}. The existence of zero points of LE means the occurrence of nonanalytic behaviors of dynamical free-energy, i.e., the rate function of LE given by $\lambda(t) = -\frac{1}{L} \ln \mathcal{L}(t)$, at these critical times. It has been shown that DQPT and the equilibrium quantum phase transition are closely related as the nonanalyticities in the rate function of LE occur for quenches crossing the quantum phase transition point^{5–7}, although a one-to-one correspondence between them does not always hold true^{9,10,35–37}. The relation between the long-time average of the LE and the ground state fidelity susceptibility^{38–42} was also unveiled recently⁴³.

In general, exact zeros of LE or nonanalyticities of dynamical free-energy only occur when the system size

tends to infinity. This is very similar to Fisher zeros of the partition function in statistical physics⁴⁴. It is well known that the Fisher zeros in a finite size system do not lie on the real temperature axis, and exact zeros only emerge in the thermodynamic limit^{44–46}. Similarly, the exact zeros of LE in a finite size quantum system can only appear in the complex time plane. When the system size tends to infinity, the zeros approach to the real time axis for quenches crossing the quantum phase transition point⁵. Now a question arise here, one may ask whether exact zeros of LE can occur in real time axis for a finite size quantum system? If the answer is yes, it seems that there exists controversy with the known results and how to understand the seeming controversy?

Aiming to answer the above questions and deepen our understanding of DQPT in the finite size systems, we shall explore the exact zeros of LE by focusing on a well-known exact solvable model, i.e., the transverse field Ising model (TFIM), which is well studied and known to exhibit DQPT in the thermodynamic limit. The existence of exact solutions enable us to analytically derive the condition for the existence of exact zeros of LE in finite size systems. For a given initial state prepared as the ground state of pre-quench Hamiltonian, our results illustrate that exact zeros of LE exist even in finite size quantum systems when the post-quench parameter takes some discrete values. These discrete parameters are found to locate in regions with the corresponding equilibrium phase different from the initial phase. As the system size increases and tends to infinity, the discrete parameters distribute continuously in the parameter regions and thus are consistent with previous results.

Further, once we know the exact zeros of LE in finite size quantum systems, it's natural to explore the minimum time of an initial state evolving to its orthogonal state which corresponds to the first time for the emergence of exact zeros of LE. The minimum time required for arriving an orthogonal quantum state is

called quantum speed limit (QSL) time^{47,48}, denoted as τ_{QSL} . The QSL time gives fundamental limit on the time scale for how fast a quantum state evolves in real-time dynamics⁴⁷⁻⁵⁹ and can be traced back to the early time when Mandelstam and Tamm studied the time-energy uncertainty in non-relativistic quantum mechanics⁶⁰. The connection of QSL to the DQPT has been discussed in the previous work⁶¹ which however only concerns on the dynamics of quantum critical state. In our paper, we shall explore both the maximum and minimum value of τ_{QSL} . For infinite size 1D TFIM, we find that the maximum value of τ_{QSL} approaches infinity, which is independent of initial state. However, the behaviour of the minimum value of τ_{QSL} is distinct if the initial state is chosen in different phase. We demonstrate that non-analytical behaviours appear in both the average of $\tau_{\text{min}}(L)$ and the variance of $\tau_{\text{min}}(L)$ when we change the prequench parameter across the static quantum phase transition point.

II. EXACT ZEROS OF LOSCHMIDT ECHO IN FINITE SIZE SYSTEMS

We consider the one-dimensional (1D) transverse field Ising model (TFIM) described by the following Hamiltonian⁶²:

$$H = -J \sum_{j=1}^L \sigma_j^x \sigma_{j+1}^x - h \sum_{j=1}^L \sigma_j^z, \quad (2)$$

where J is the nearest-neighbor spin coupling, h is the external magnetic field along the z axis and the periodical boundary condition $\sigma_{L+1}^x = \sigma_1^x$ is assumed. The three Pauli matrices are σ_j^α ($\alpha = x, y, z$), $j = 1, \dots, L$ with L denoting total number of lattice sites. The TFIM fulfills a duality relation^{63,64}: $UH(h)U^{-1} = H(1/h)$. By using the Jordan-Wigner transformation, the even-parity and odd-parity of the TFIM with periodical boundary condition can be mapping to the anti-periodical Kitaev chain and periodical Kitaev chain, respectively. Then we can write the Hamiltonian in the fermion representation as

$$H = -J \sum_{j=1}^{L-1} \left(c_j^\dagger c_{j+1} + c_j^\dagger c_{j+1}^\dagger + \text{H.c.} \right) - 2h \sum_{j=1}^L c_j^\dagger c_j \pm (c_L^\dagger c_1 + c_L^\dagger c_1^\dagger + \text{H.c.}), \quad (3)$$

where plus sign or minus sign of h is corresponding to the even-parity or odd-parity. For convenience, we shall set $J = 1$ as the unit of energy in the following calculation.

It is convenient to diagonalize the Hamiltonian (3) in the momentum space by using the Fourier transform $c_j^\dagger = \frac{1}{\sqrt{L}} \sum_k e^{ikj} c_k^\dagger$. Here values of k should be chosen in set $\mathcal{K}_{\text{PBC}} = \{k = \frac{2\pi m}{L} | m = -L/2 + 1, \dots, 0, \dots, L/2\}$ for periodical boundary condition (PBC) and $\mathcal{K}_{\text{aPBC}} = \{k = \pm \frac{\pi(2m-1)}{L} | m = 1, \dots, L/2\}$ for anti-periodical boundary condition (aPBC). In the following

discussion, we focus on the even site of lattice with even parity which is corresponding to aPBC. It should be noted that all terms of Hamiltonian come into pairs $(k, -k)$ for aPBC. Define the positive k values as $\mathcal{K}_{\text{aPBC}}^+ = \{k = \frac{\pi(2m-1)}{L} | m = 1, \dots, L/2\}$. Then the Hamiltonian in momentum space is

$$H = -2 \sum_{k \in \mathcal{K}_{\text{aPBC}}^+} \left[(\cos k + h) (c_k^\dagger c_k - c_{-k} c_{-k}^\dagger) + (i \sin k c_k^\dagger c_{-k}^\dagger + \text{H.c.}) \right], \quad (4)$$

By using the Bogoliubov transformation

$$\begin{aligned} \beta_k &= \cos \theta_k c_k + i \sin \theta_k c_{-k}^\dagger, \\ \beta_{-k}^\dagger &= i \sin \theta_k c_k + \cos \theta_k c_{-k}^\dagger, \end{aligned}$$

where $\frac{\epsilon_k}{E_k} = \cos 2\theta_k$ and $\frac{\zeta_k}{E_k} = \sin 2\theta_k$ with $\epsilon_k = -\cos k - h$ and $\zeta_k = -\sin k$. we arrive at a Hamiltonian given by^{62,65,66}

$$H = 2 \sum_{k \in \mathcal{K}_{\text{aPBC}}^+} \left(E_k \beta_k^\dagger \beta_k - E_k \beta_{-k} \beta_{-k}^\dagger \right), \quad (5)$$

where $E_k = \sqrt{\epsilon_k^2 + \zeta_k^2}$.

Then we consider the quench dynamic driven by the transverse field h which can be described by $h(t) = h_i \Theta(-t) + h_f \Theta(t)$. The analytical formula of Loschmidt echo has the form

$$\mathcal{L}(t) = \prod_{k \in \mathcal{K}_{\text{aPBC}}^+} [1 - \sin^2(2\delta\theta_k) \sin^2(2E_k f t)], \quad (6)$$

where $\delta\theta_k = \theta_{kf} - \theta_{ki}$ with θ_{ki} is Bogoliubov angle of prequench Hamiltonian and θ_{kf} is Bogoliubov angle of postquench Hamiltonian, and E_{kf} is the energy of postquench Hamiltonian. To ensure $\mathcal{L}(t) = 0$, we must have $\sin^2(2\delta\theta_k) = 1$, which gives rise to the following constraint relation

$$h_f = -\frac{1 + h_i \cos k}{h_i + \cos k}. \quad (7)$$

For a finite size system, the momentum k takes discrete values. Given the prequench parameter h_i , we can get a series of h_f determined by Eq.(7) for various k . When the postquench parameter takes these discrete values, we have $\mathcal{L}(t) = 0$ at

$$t = t_n^* = \frac{\pi}{2E_{kf}} (n + 1/2), \quad (8)$$

with

$$E_{kf} = \sqrt{(\cos k + h_f)^2 + (\sin k)^2}, \quad (9)$$

i.e., there exist exact zeros of LE as long as Eq.(7) is fulfilled. According to Eq.(7), if $h_i \in (-1, 1)$, the exact zeros of LE emerge only for $h_f \in (-\infty, -1) \cup (1, \infty)$. For

the 1D transverse field Ising chain, we can prove that the Loschmidt echo fulfills the following dynamical duality relation

$$\mathcal{L}(h_i, h_f, t) = \mathcal{L}\left(\frac{1}{h_i}, \frac{1}{h_f}, h_f t\right). \quad (10)$$

Due to the existence of dynamical duality relation (see appendix for details), we only need to consider the case of $h_i \in (-1, 1)$ as the cases $h_i \in (-\infty, -1)$ and $h_i \in (1, \infty)$ can be obtained by using the dynamical duality relation.

As displayed in Fig.1(a) for the system with lattice size $L = 14$, for a given h_i , only $L/2$ discrete values of h_f satisfy Eq.(7). Continuously varying h_i leads to the formation of a series of curves in the parameter space spanned by h_i and h_f . And those curves become more and more dense as we increase the lattice size, as shown in Fig.1(b) for the system with $L = 400$. To characterize the average distance between neighboring curves, we define the quantity $\bar{\Delta}$ as

$$\bar{\Delta} = \frac{1}{L-1} \sum_{k=\frac{1-L}{2}\pi}^{\frac{L-3}{2}\pi} \left| h_f\left(k + \frac{2\pi}{L}\right) - h_f(k) \right|, \quad (11)$$

where $h_f(k)$ is the solution of Eq.(7) for a k mode. In the thermodynamic limit we can turn the sum into an integral and it could be found that $\bar{\Delta}$ is approximately equal to $4/L$ which approaches to 0 as $L \rightarrow \infty$. This is also confirmed by the numerical result as displayed in Fig.2(a). Therefore the discrete h_f tend to distribute continuously in thermodynamic limit, which is consistent with the general knowledge about the DQPT that zeros of LE shall appear when we quench the system across the critical point.

If we quench the system to the critical point $h_f = 1$ (-1), from Eq.(7), we can see that no exact zeros of LE are available unless the initial state is prepared in the other critical point $h_i = -1$ (1). Interesting, if we restrict $h_i \geq 0$ and $h_f \geq 0$, no exact zero of Loschmidt echo can be found if the value of h_i or h_f is in the interval $(-\cos \frac{L-1}{L}\pi, -\sec \frac{L-1}{L}\pi)$ for the finite size system. The interval $(-\cos \frac{L-1}{L}\pi, -\sec \frac{L-1}{L}\pi) \approx (1 - \frac{1}{2}(\frac{\pi}{L})^2, 1 + \frac{1}{2}(\frac{\pi}{L})^2)$ is around the critical point $h_c = 1$ and the boundary of the interval are reciprocal due to the existence of dynamical duality for the TFIM. Moreover, we can define a quantity $\Delta_c(h_i)$ which represents the shortest distant between $h_f = 1$ and the solution of Eq.(7) for arbitrary value of h_i . The numerical result of $\Delta_c(h_i)$ is shown in Fig.2(b) for $h_i = -1.5, -0.2, 0.6, 2$ represented by different marks. The approximate formula of $\Delta_c(h_i)$ for large L can be derived from Eq.(7), which reads as

$$\Delta_c(h_i) = \frac{\alpha(h_i)}{L^2}, \quad (12)$$

where $\alpha(h_i) = \frac{\pi^2(1+h_i)}{2(1-h_i)}$. The results of Eq.(12) for $h_i = -1.5, -0.2, 0.6, 2$ are shown in Fig.(2)(b) which are

denoted by black dashed lines. So, if we quench the system from arbitrary value of h_i except -1 to h_f near the critical point, then there exists a region in which no exact zeros of LE are available for finite size system. The width of this region is dependent on h_i and $\Delta_c(h_i) \rightarrow 0$ in the thermodynamic limit for any h_i . Together with the result of $\bar{\Delta} \rightarrow 0$, we can see that exact zeros of LE would exist so long as we quench across the critical point for the infinite size system, in agreement with the previous work. The result of the shortest distant between $h_f = -1$ and the solution of Eq.(7) for arbitrary value of h_i is similar to Eq.(12).

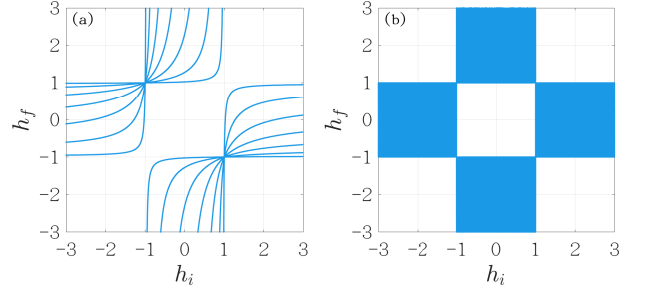


Figure 1. The combination of h_i and h_f which fulfill Eq.(7). (a) $L = 14$ and (b) $L = 400$.

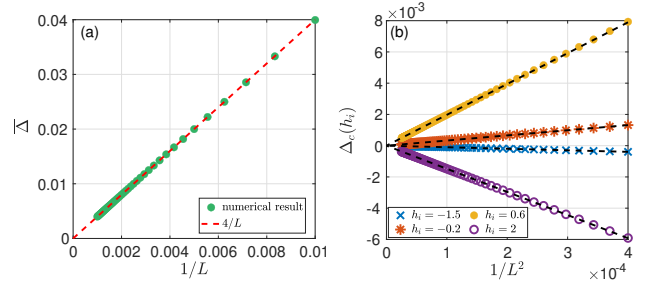


Figure 2. (a) Green dots are the numerical results of Eq.(11) for finite size systems. Red dashed line is the result in the large size limit $\bar{\Delta} \approx 4/L$. We set prequench parameter as $h_i = 1.5$. (b) The $\Delta_c(h_i)$ with respect to $1/L^2$ for different value of h_i . The discrete marks are the numerical results and the dashed lines are the results of Eq.(12).

III. QUANTUM SPEED LIMIT TIME FOR DYNAMICAL QUANTUM PHASE TRANSITION

From previous section, we know that there exist exact zeros of LE as we quench the ground state across the static phase transition point. It is known that the quantum speed limit (QSL) time is the minimal time for the evolution of an initial state to its orthogonal state, and thus the first time for the emergence of exact zero of LE

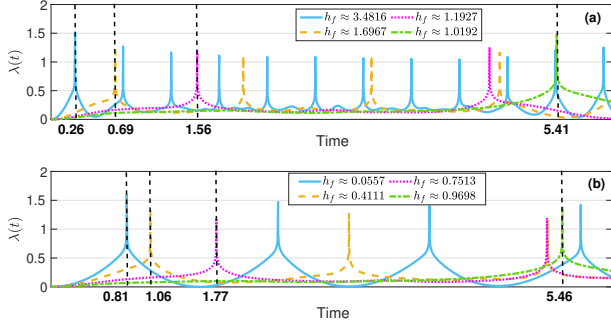


Figure 3. Rate function $\lambda(t)$ for $L = 22$. Black dashed lines guide the first time of the exact zeros of LE appeared for every h_f . The prequench parameter is (a) $h_i = 0.3$ and (b) $h_i = 2$.

gives the QSL time, i.e.,

$$\tau_{\text{QSL}} = \frac{\pi}{4E_{kf}}. \quad (13)$$

According to Eq.(9), the QSL time is dependent on the values h_f .

As displayed in Fig.3 for the system with $L = 22$, we show that series of divergence points of rate function, corresponding to exact zeros of LE, appear in the real time axis. The QSL time corresponds to the first divergence point of rate function, which is labeled by black dashed line. To see the dependence of τ_{QSL} on h_f , we plot rate function versus t for all permitted $h_f > 0$ determined by Eq.(7). Particularly, we denote the maximal value of quantum speed limit time as $\tau_{\text{max}} = \max[\tau_{\text{QSL}}]$. It is found that τ_{max} is corresponding to the quench process with the postquench parameter closest to $h_c = 1$. From the analytical result Eq.(7) and the formula of E_{kf} , it follows that $E_{kf} \approx \frac{\pi}{L}$ is minima if $k = \frac{\pi}{L}$ or $k = \frac{L-1}{L}\pi$. According to Eq.(7), it should also be noted that the mode $k = \frac{\pi}{L}$ and $k = \frac{L-1}{L}\pi$ is corresponding to h_f close to -1 and 1 for finite size system, respectively. Then we have $\tau_{\text{max}} \approx \frac{L}{4}$ which can be regarded as an upper bound of QSL time. In the thermodynamic limit, $k \rightarrow 0$ and $k \rightarrow \pi$ is corresponding to $h_f \rightarrow -1$ and $h_f \rightarrow 1$, respectively. When $L \rightarrow \infty$, we have $\tau_{\text{max}} \rightarrow \infty$ with $|h_f| \rightarrow 1$. This means that we can not observe the DQPT in a finite time if we quench the system from a non-critical phase to the critical phase with $|h_f| = 1$.

For any ground state of 1D TFIM, it is also interesting to ask how fast could the ground state achieve to its orthogonal state as we quench the parameter of the system? The answer of the question is given by the minimal value of QSL time denoted as $\tau_{\text{min}} = \min[\tau_{\text{QSL}}]$. In Fig.4, we demonstrate the behaviour of $\tau_{\text{min}}(L)$ for various prequench parameters h_i as the system size increases. It could be found that if the initial state lies in the paramagnetic phase (Fig.4(a)), τ_{min} would approach to zero as the system size increase. However, τ_{min} would approach to some finite values if the initial state lies in the ferromagnetic phase (Fig.4(b)).

To get a better understanding, now we discuss two limiting cases. One is the initial state chosen in the ferromagnetic phase, i.e., the ground state of the prequench Hamiltonian with $h_i = \infty$. It can be seen that τ_{min} is corresponding to the maximal value of $E_{kf} = \sqrt{(\cos k + h_f)^2 + \sin^2 k}$ with h_f fulfilling Eq.(7). For $h_i = \infty$, the maximal value of E_{kf} in the thermodynamic limit is $E_{kf} = 1$ corresponding to $k = \pi/2$, so we have $\tau_{\text{min}} = \pi/4$. This limiting case can be observed in Fig.4(b) for $h_i = 1000$, where the black dashed line guides the value of $\pi/4$. On the contrary, if we consider the prequench Hamiltonian lying in the paramagnetic phase with $h_i = 0$. From Eq.(7), we have $h_f = -1/\cos k$, and it follows that the maximal value of E_{kf} is $E_{kf} = \infty$ corresponding to $k = \pi/2$, which means $\tau_{\text{min}} = 0$ in the thermodynamic limit. For the finite size system, k can be exactly equal to $\frac{\pi}{2}$ if $\text{mod}(L, 4) = 2$, so we have $\tau_{\text{min}} = 0$. Otherwise, $k = \frac{\pi}{2} + \frac{\pi}{L}$ is the mode closest to $\frac{\pi}{2}$ for $\text{mod}(L, 4) = 0$. In this case, we have $h_f \approx \frac{L}{\pi}$ for $L \rightarrow \infty$ and the maximal value of $E_{kf} \approx \frac{L}{\pi}$ with $k = \frac{\pi}{2} + \frac{\pi}{L}$. Then we have $\tau_{\text{QSL}} \approx \frac{\pi^2}{4L}$ which is illustrated in Fig.4(a) by the green dashed line and it is shown that the asymptotic behavior of τ_{QSL} is captured by the line of $\frac{\pi^2}{4L}$ for $|h_i| < 1$.

From the previous work^{50,52,60}, we know that the lower bound of QSL time can be given by Mandelstam–Tamm bound τ_{MT} :

$$\tau_{\text{QSL}} \geq \tau_{\text{MT}} \equiv \frac{\pi \hbar}{2\Delta E}, \quad (14)$$

where $(\Delta E)^2 = \langle \psi_i | H_f^2 | \psi_i \rangle - (\langle \psi_i | H_f | \psi_i \rangle)^2$ with H_f denotes the postquench Hamiltonian. Next, we consider the two cases discussed above. For the case with ferromagnetic initial state $|\psi_i\rangle = \otimes_{j=1}^L |\uparrow\rangle_j$ and the postquench Hamiltonian $H_f = -\sum_{j=1}^L \sigma_j^x \sigma_{j+1}^x$ ($h_f = 0$), we have $\Delta E = L$ due to $\langle \psi_i | H_f^2 | \psi_i \rangle = L$ and $\langle \psi_i | H_f | \psi_i \rangle = 0$. So the Mandelstam–Tamm bound is $\tau_{\text{MT}} \rightarrow 0$ in the thermodynamical limit. For the other case with the paramagnetic initial state $|\psi_i\rangle = \frac{\sqrt{2}}{2}(\otimes_{j=1}^L |\rightarrow\rangle_j + \otimes_{j=1}^L |\leftarrow\rangle_j)$ and $H_f = -h_f \sum_{j=1}^L \sigma_j^z$ with $h_f \rightarrow \infty$, we have $\Delta E \rightarrow \infty$ and $\tau_{\text{MT}} \rightarrow 0$. It can be seen that the Mandelstam–Tamm bound of QSL time is equal to zero for both two cases. Compare with our exact result of τ_{QSL} , it can be found that the Mandelstam–Tamm bound τ_{MT} is tight if the prequench Hamiltonian lies in the paramagnetic phase.

To see clearly how $\tau_{\text{min}}(L)$ changes with h_i , we can calculate the mean value of $\tau_{\text{min}}(L)$ numerically from L_{min} to L_{max} and denote it as:

$$\bar{\tau}_{\text{min}} = \frac{1}{L_{\text{max}} - L_{\text{min}}} \sum_{L=L_{\text{min}}}^{L_{\text{max}}} \tau_{\text{min}}(L). \quad (15)$$

Meanwhile, we can also calculate the variance of $\tau_{\text{min}}(L)$

defined by:

$$\sigma_{\tau_{min}}^2 = \frac{1}{L_{max} - L_{min}} \sum_{L=L_{min}}^{L_{max}} [\tau_{min}^2(L) - \bar{\tau}_{min}^2]. \quad (16)$$

We count from $L_{min} = 10$ to $L_{max} = 10000$ and show the numerical results of $\bar{\tau}_{min}$ and $\sigma_{\tau_{min}}^2$ with respect to prequench parameter h_i in Fig.5(a) and (b), respectively. It can be observed that both $\bar{\tau}_{min}$ and $\sigma_{\tau_{min}}^2$ have an abrupt change at $h_i = 1$ which corresponds to the static quantum phase transition point in the thermodynamic limit. The fluctuation of energy can be evidenced in $\sigma_{\tau_{min}}^2$ (Fig.5(b)) which remains non-zero value as $|h_i| < 1$ and diverges as $|h_i|$ approaches 1. The non-analytical behaviours appearing in the change of prequench parameter across the static quantum phase transition point indicates clearly the minima of QSL time relies on the choice of initial states.

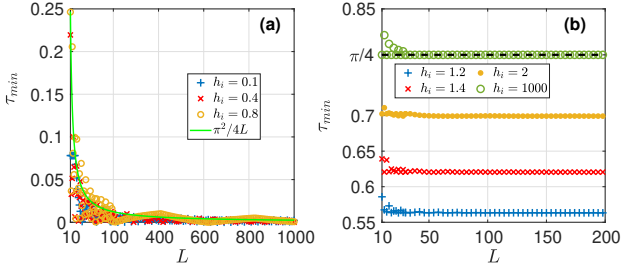


Figure 4. $\tau_{min}(L)$ versus system size L . The prequench parameter is (a) $|h_i| < 1$ and (b) $|h_i| > 1$.

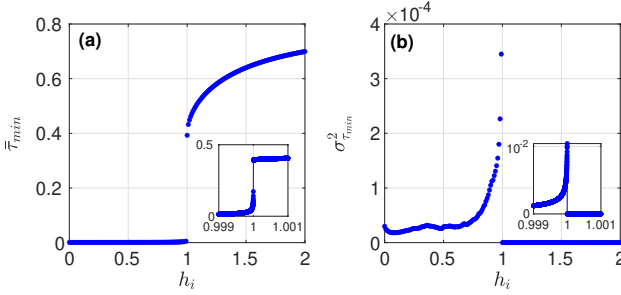


Figure 5. (a) $\bar{\tau}_{min}$ with respect to h_i ; (b) $\sigma_{\tau_{min}}^2$ with respect to h_i . Here we count the size of system from $L_{min} = 10$ to $L_{max} = 10000$.

IV. SUMMARY

In summary, we have analytically calculated the exact zeros of the LE for the 1D TFIM and shown that there exist exact zeros of LE even for the finite size quantum system. We have illustrated that our analytical result is in agreement with previous work in the thermodynamic limit. For finite size system of 1D TFIM, we have examined the quantum speed limit time and studied the

behaviors of the maximum and minimum values of quantum speed limit time. From our analytical result in thermodynamic limit, it is shown that no DQPT occurs in a finite time if we quench from non-critical system to critical system due to corresponding τ_{max} is approaching infinity. We have also illustrated the existence of non-analytical behaviors in both the average of $\tau_{min}(L)$ and the variance of $\tau_{min}(L)$ when we change the parameter of prequench Hamiltonian across the static critical point.

ACKNOWLEDGMENTS

This work is supported by NSFC under Grants No.11974413 and the Strategic Priority Research Program of Chinese Academy of Sciences under Grant No. XDB33000000.

Appendix A: The dynamical duality of the Loschmidt echo

For quantum TFIM, the Loschmidt echo can be represented as

$$\mathcal{L}(J_i, J_f, h_i, h_f, t) = \prod_k \mathcal{L}_k(J_i, J_f, h_i, h_f, t), \quad (A1)$$

where the k -component of the Loschmidt echo is

$$\mathcal{L}_k(J_i, J_f, h_i, h_f, t) = 1 - \sin^2(2\delta\theta_k) \sin^2(2E_{kf}t). \quad (A2)$$

Here we have

$$\begin{aligned} \sin^2(2\delta\theta_k) &= \left(\frac{\zeta_f}{E_f} \frac{\epsilon_i}{E_i} - \frac{\epsilon_f}{E_f} \frac{\zeta_i}{E_i} \right)^2 \\ &= \frac{(\zeta_f \epsilon_i - \epsilon_f \zeta_i)^2}{(\epsilon_i^2 + \zeta_i^2)(\epsilon_f^2 + \zeta_f^2)} \\ &= \frac{(J_f h_i - J_i h_f)^2 \sin^2 k}{(J_i^2 + 2J_i h_i \cos k + h_i^2)(J_f^2 + 2J_f h_f \cos k + h_f^2)}, \end{aligned}$$

and

$$\sin^2(2E_{kf}t) = \sin^2\left(2t\sqrt{J_f^2 + 2J_f h_f \cos k + h_f^2}\right).$$

After a dual transformation: $J \rightarrow 1/J$ and $h \rightarrow 1/h$, the k -component of Loschmidt echo of the dual model can be written as

$$\mathcal{L}_k\left(\frac{1}{J_i}, \frac{1}{J_f}, \frac{1}{h_i}, \frac{1}{h_f}, t\right) = 1 - \sin^2(2\delta\tilde{\theta}_k) \sin^2(2\tilde{E}_{kf}t), \quad (A3)$$

with

$$\begin{aligned}
& \sin^2(2\delta\tilde{\theta}_k) \\
&= \frac{\left(\frac{1}{J_f h_i} - \frac{1}{J_i h_f}\right)^2 \sin^2 k}{\left(\frac{1}{J_i^2} + 2\frac{1}{J_i h_i} \cos k + \frac{1}{h_i^2}\right) \left(\frac{1}{J_f^2} + 2\frac{1}{J_f h_f} \cos k + \frac{1}{h_f^2}\right)} \\
&= \frac{(J_i h_f - J_f h_i)^2 \sin^2 k}{(h_i^2 + 2J_i h_i \cos k + J_i^2) (h_f^2 + 2J_f h_f \cos k + J_f^2)} \\
&= \sin^2(2\delta\theta_k),
\end{aligned}$$

and

$$\begin{aligned}
& \sin^2(2\tilde{E}_{kf}t) \\
&= \sin^2\left(2t\sqrt{\frac{1}{J_f^2} + 2\frac{1}{J_f h_f} \cos k + \frac{1}{h_f^2}}\right) \\
&= \sin^2\left(2\sqrt{J_f^2 + 2J_f h_f \cos k + h_f^2} \frac{t}{J_f h_f}\right) \\
&= \sin^2\left(2E_{kf} \frac{t}{J_f h_f}\right).
\end{aligned}$$

We can observe that

$$\mathcal{L}_k\left(\frac{1}{J_i}, \frac{1}{J_f}, \frac{1}{h_i}, \frac{1}{h_f}, t\right) = \mathcal{L}_k(J_i, J_f, h_i, h_f, \frac{t}{J_f h_f}), \quad (\text{A4})$$

In a more convenient form, it can be written as

$$\mathcal{L}_k\left(\frac{1}{J_i}, \frac{1}{J_f}, \frac{1}{h_i}, \frac{1}{h_f}, J_f h_f t\right) = \mathcal{L}_k(J_i, J_f, h_i, h_f, t). \quad (\text{A5})$$

For the case of $J_i = J_f = 1$ in the main text, we have

$$\mathcal{L}_k\left(\frac{1}{h_i}, \frac{1}{h_f}, h_f t\right) = \mathcal{L}_k(h_i, h_f, t), \quad (\text{A6})$$

which gives rise to the dynamical dual relation Eq.(10) directly.

* Corresponding author: schen@iphy.ac.cn

- ¹ H. Bernien, S. Schwartz, A. Keesling, H. Levine, A. Omran, H. Pichler, S. Choi, A. S. Zibrov, M. Endres, M. Greiner et al., Probing many-body dynamics on a 51-atom quantum simulator, *Nature* (London) **551**, 579 (2017).
- ² A. Omran, H. Levine, A. Keesling, G. Semeghini, T. T. Wang, S. Ebadi, H. Bernien, A. S. Zibrov, H. Pichler, S. Choi et al., Generation and manipulation of Schrödinger cat states in Rydberg atom arrays, *Science* **365**, 570 (2019).
- ³ D. Bluvstein, A. Omran, H. Levine, A. Keesling, G. Semeghini, S. Ebadi, T. T. Wang, A. A. Michailidis, N. Maskara, W. W. Ho et al., Controlling many-body dynamics with driven quantum scars in Rydberg atom arrays, arXiv:2012.12276.
- ⁴ S. Ebadi, T. T. Wang, H. Levine, A. Keesling, G. Semeghini, A. Omran, D. Bluvstein, R. Samajdar, H. Pichler, Wen Wei Ho et al., Quantum phases of matter on a 256-Atom programmable quantum simulator, arXiv:2012.12281.
- ⁵ M. Heyl, A. Polkovnikov, S. Kehrein, dynamical quantum phase transitions in the transverse-field Ising model, *Phys. Rev. Lett.* **110**, 135704 (2013).
- ⁶ C. Karrasch and D. Schuricht, Dynamical phase transitions after quenches in nonintegrable models, *Phys. Rev. B* **87**, 195104 (2013).
- ⁷ J. M. Hickey, S. Genway, and J. P. Garrahan, Dynamical phase transitions, time-integrated observables, and geometry of states, *Phys. Rev. B* **89**, 054301 (2014).
- ⁸ E. Canovi, P. Werner, and M. Eckstein, First-order dynamical phase transitions, *Phys. Rev. Lett.* **113**, 265702 (2014).
- ⁹ F. Andraschko and J. Sirker, Dynamical quantum phase transitions and the Loschmidt echo: A transfer matrix ap-

- proach, *Phys. Rev. B* **89**, 125120 (2014).
- ¹⁰ M. Schmitt and S. Kehrein, Dynamical quantum phase transitions in the Kitaev honeycomb model, *Phys. Rev. B* **92**, 075114 (2015).
- ¹¹ M. Marcuzzi, E. Levi, S. Diehl, J. P. Garrahan, and I. Lesanovsky, Universal nonequilibrium properties of dissipative Rydberg gases, *Phys. Rev. Lett.* **113**, 210401 (2014).
- ¹² M. Heyl, Dynamical Quantum phase transitions in systems with broken-symmetry phases, *Phys. Rev. Lett.* **113**, 205701 (2014).
- ¹³ M. Heyl, Scaling and universality at dynamical quantum phase transitions, *Phys. Rev. Lett.* **115**, 140602 (2015).
- ¹⁴ S. Vajna and B. Dóra, Topological classification of dynamical phase transitions, *Phys. Rev. B* **91**, 155127 (2015).
- ¹⁵ N. O. Abeling and S. Kehrein, Quantum quench dynamics in the transverse field Ising model at nonzero temperatures, *Phys. Rev. B* **93**, 104302 (2016).
- ¹⁶ J. C. Budich and M. Heyl, Dynamical topological order parameters far from equilibrium, *Phys. Rev. B* **93**, 085416 (2016).
- ¹⁷ A. A. Zvyagin, Dynamical quantum phase transitions (Review Article), *Fiz. Nizk. Temp. (Kiev)* **42**, 1240 (2016) [*Low Temp. Phys.* **42**, 971 (2016)].
- ¹⁸ M. Heyl, Dynamical quantum phase transitions: a review, *Rep. Prog. Phys.* **81**, 054001 (2018).
- ¹⁹ C. Yang, Y. Wang, P. Wang, X. Gao and S. Chen, Dynamical signature of localization-delocalization transition in a one-dimensional incommensurate lattice, *Phys. Rev. B* **95**, 184201 (2017).
- ²⁰ M. Heyl, F. Pollmann, and B. Dóra, Detecting equilibrium and dynamical quantum phase transitions in Ising chains via out-of-time-ordered correlators, *Phys. Rev. Lett.* **121**,

- 016801 (2018).
- ²¹ B. Mera, C. Vlachou, N. Paunković, V. R. Vieira, and O. Viyuela, Dynamical phase transitions at finite temperature from fidelity and interferometric Loschmidt echo induced metrics, *Phys. Rev. B* **97**, 094110 (2018).
 - ²² P. Jurcevic, H. Shen, P. Hauke, C. Maier, T. Brydges, C. Hempel, B. P. Lanyon, M. Heyl, R. Blatt, and C. F. Roos, Direct observation of dynamical quantum phase transitions in an interacting many-body system, *Phys. Rev. Lett.* **119**, 080501 (2017).
 - ²³ X.-Y. Guo, C. Yang, Y. Zeng, Y. Peng, H.-K. Li, H. Deng, Y.-R. Jin, S. Chen, D. Zheng, and H. Fan, Observation of a dynamical quantum phase transition by a superconducting qubit simulation, *Phys. Rev. Applied* **11**, 044080 (2019).
 - ²⁴ N. Fläschner, D. Vogel, M. Tarnowski, B. S. Rem, D.-S. Lühmann, M. Heyl, J. C. Budich, L. Mathey, K. Sengstock, and C. Weitenberg, Observation of dynamical vortices after quenches in a system with topology, *Nat. Phys.* **14**, 265 (2018).
 - ²⁵ K. Wang, X. Qiu, L. Xiao, X. Zhan, Z. Bian, W. Yi, and P. Xue, Simulating dynamic quantum phase transitions in photonic quantum walks, *Phys. Rev. Lett.* **122**, 020501 (2019).
 - ²⁶ X. Nie, B.-B. Wei, X. Chen, Z. Zhang, X. Zhao, C. Qiu, Y. Tian, Y. Ji, T. Xin, D. Lu, and J. Li, Experimental Observation of Equilibrium and Dynamical Quantum Phase Transitions via Out-of-Time-Ordered Correlators, *Phys. Rev. Lett.* **124**, 250601(2020).
 - ²⁷ G. Sun, B.-B. Wei, Dynamical quantum phase transitions in a spin chain with deconfined quantum critical points, *Phys. Rev. B* **102**, 094302 (2020).
 - ²⁸ T. Gorin, T. Prosen, T. H. Seligman, and M. Znidaric, Dynamics of Loschmidt echoes and fidelity decay, *Phys. Rep.* **435**, 33 (2006).
 - ²⁹ A. Peres, Stability of quantum motion in chaotic and regular systems, *Phys. Rev. A* **30**, 1610 (1984).
 - ³⁰ R. A. Jalabert and H. M. Pastawski, Environment-independent decoherence rate in classically chaotic systems, *Phys. Rev. Lett.* **86**, 2490 (2001).
 - ³¹ A. E. Martinez, A. C. Muschik, P. Schindler, D. Nigg, A. Erhard, M. Heyl, P. Hauke, M. Dalmonte, T. Monz, P. Zoller and R. Blatt, Real-time dynamics of lattice gauge theories with a few-qubit quantum computer, *Nature* **534**, 516 (2016).
 - ³² J. Schwinger, On gauge invariance and vacuum polarization, *Phys. Rev.* **82**, 664 (1951).
 - ³³ P. Talkner, E. Lutz and P. Hänggi, Fluctuation theorems: Work is not an observable, *Phys. Rev. E* **75**, 050102 (2007).
 - ³⁴ T. Palmai, Edge exponents in work statistics out of equilibrium and dynamical phase transitions from scattering theory in one-dimensional gapped systems, *Phys. Rev. B* **92**, 235433 (2015).
 - ³⁵ S. Vajna and B. Dora, Disentangling dynamical phase transitions from equilibrium phase transitions, *Phys. Rev. B* **89**, 161105 (2014).
 - ³⁶ S. Sharma, S. Suzuki, and A. Dutta, Quenches and dynamical phase transitions in a nonintegrable quantum Ising model, *Phys. Rev. B* **92**, 104306 (2015).
 - ³⁷ R. Jafari, Dynamical quantum phase transition and quasi particle excitation, *Sci. Rep.* **9**, 2871 (2019).
 - ³⁸ P. Zanardi and N. Paunković, Ground state overlap and quantum phase transitions, *Phys. Rev. E* **74**, 031123 (2006).
 - ³⁹ W. L. You, Y. W. Li, and S. J. Gu, Fidelity, dynamic structure factor, and susceptibility in critical phenomena, *Phys. Rev. E* **76**, 022101 (2007).
 - ⁴⁰ S. Chen, L. Wang, Y. Hao, and Y. Wang, Intrinsic relation between ground-state fidelity and the characterization of a quantum phase transition, *Phys. Rev. A* **77**, 032111 (2008).
 - ⁴¹ S. Chen, L. Wang, S. J. Gu, and Y. Wang, Fidelity and quantum phase transition for the Heisenberg chain with next-nearest-neighbor interaction, *Phys. Rev. E* **76**, 061108 (2007).
 - ⁴² H. Q. Zhou and J. P. Barjaktarevic, Fidelity and quantum phase transitions, *J. Phys. A* **41**, 412001 (2008).
 - ⁴³ B. Zhou, C. Yang, and S. Chen, Signature of a nonequilibrium quantum phase transition in the long-time average of the Loschmidt echo, *Phys. Rev. B* **100**, 184313 (2019).
 - ⁴⁴ M. E. Fisher, *Boulder Lectures in Theoretical Physics* (University of Colorado, Boulder, 1965), Vol. 7.
 - ⁴⁵ C. Yang and T. Lee, Statistical theory of equations of state and phase transitions. I. Theory of condensation, *Phys. Rev.* **87**, 404 (1952).
 - ⁴⁶ W. van Saarloos and D. Kurtze, Location of zeros in the complex temperature plane: absence of Lee-Yang theorem, *J. Phys. A* **17**, 1301 (1984).
 - ⁴⁷ V. Giovannetti, S. Lloyd, and L. Maccone, Quantum limits to dynamical evolution, *Phys. Rev. A* **67**, 052109 (2003).
 - ⁴⁸ V. Giovannetti, S. Lloyd, and L. Maccone, The speed limit of quantum unitary evolution, *J. Opt. B: Quan. Semi. Opt.* **6**, S807 (2004).
 - ⁴⁹ G. N. Fleming, A Unitarity bound on the evolution of non-stationary states, *Nuovo Cimento A* **16**, 232 (1973).
 - ⁵⁰ K. Bhattacharyya, Quantum decay and the Mandelstam-Tamm-energy inequality, *J. Phys. A: Math. Gen.* **16**, 2993 (1983).
 - ⁵¹ J. Anandan and Y. Aharonov, Geometry of quantum evolution, *Phys. Rev. Lett.* **65**, 1697 (1990).
 - ⁵² Lev Vaidman, Minimum time for the evolution to an orthogonal quantum state, *Am. J. Phys.* **60**, 182 (1992).
 - ⁵³ N. Margolus and L. B. Levitin, The maximum speed of dynamical evolution, *Phys. D* **120**, 188 (1998).
 - ⁵⁴ J. Uffink, The rate of evolution of a quantum state, *Am. J. Phys.* **61**, 935 (1993).
 - ⁵⁵ P. Pfeifer, How fast can a quantum state change with time?, *Phys. Rev. Lett.* **70**, 3365 (1993).
 - ⁵⁶ N. Margolus and L. B. Levitin, The maximum speed of dynamical evolution, *Physica (Amsterdam)* **120D**, 188 (1998).
 - ⁵⁷ L. B. Levitin and T. Toffoli, Fundamental limit on the rate of quantum dynamics: The unified bound is tight, *Phys. Rev. Lett.* **103**, 160502 (2009).
 - ⁵⁸ P. M. Poggi, F. C. Lombardo, and D. A. Wisniacki, Quantum speed limit and optimal evolution time in a two-level system, *Europhys. Lett.* **104**, 40005 (2013).
 - ⁵⁹ T. Fogarty, S. Deffner, T. Busch and S. Campbell, Orthogonality catastrophe as a consequence of the quantum speed limit, *Phys. Rev. Lett.* **124**, 110604 (2020).
 - ⁶⁰ L. Mandelstam and I. Tamm, The uncertainty relation between energy and time in nonrelativistic quantum mechanics, *J. Phys. (Moscow)* **9**, 249 (1945).
 - ⁶¹ M. Heyl, Quenching a quantum critical state by the order parameter: Dynamical quantum phase transitions and quantum speed limits, *Phys. Rev. B* **95**, 060504 (2017).
 - ⁶² P. Pfeuty, The one-dimensional Ising model with a transverse field, *Ann. Phys. (N.Y.)* **57**, 79 (1970).

- ⁶³ E. Fradkin and L. Susskind, Order and disorder in gauge systems and magnets, *Phys. Rev. D* **17**, 2637 (1978).
- ⁶⁴ L. Zhang, *Phys. Rev. Lett.* **123**, 230601 (2019).
- ⁶⁵ E. Lieb, T. Schultz, and D. Mattis, Two soluble models of an antiferromagnetic chain, *Ann. Phys. (NY)* **16**, 407 (1961).
- ⁶⁶ G. B. Mbeng, A. Russomanno, G. E. Santoro, The quantum Ising chain for beginners, arXiv:2009.09208v1.